Showcasing work from the African Centre of Excellence in Future Energies and Electrochemical Systems at the Federal University of Technology Owerri, Nigeria. The project is led by Professor Emeka E. Oguzie, with Dr. Elias E. Elemike (Federal University of Petroleum Resources, Nigeria) and Dr. Christian O. Dimkpa (Connecticut Agricultural Experiment Station, USA) as collaborators.

Morphological and chemical profiling of biochar derived from invasive aquatic weed towards bio-nanofertilizer development

This study explores the structural and chemical characteristics of biochar produced from water hyacinth, an invasive aquatic weed. Advanced analyses reveal the biochar's porous architecture, surface properties, and elemental makeup, assessing its viability as a sustainable precursor for bio-nanofertilizers, aligned with the International Biochar Initiative's framework. The findings pave the way for transforming an ecological nuisance into high-value agro-materials, driving eco-smart fertilizer innovation in sustainable agriculture.

Image reproduced by permission of Emeka E. Oguzie from *RSC Sustainability,* 2025, **3**, 3947.

Image created with Biorender.com.

As featured in:

See Christian O. Dimkpa, Emeka Emmanuel Oguzie *et al.*, *RSC Sustainability*, 2025, **3**, 3947.

ROYAL SOCIETY OF **CHEMISTRY**

rsc.li/rscsus

Check for updates

Morphological and chemical profiling of biochar derived from invasive aquatic weed towards bio-nanofertilizer development†

Adewale Tolulope Irewale, [ab] Elias Emeka Elemike, [ac] Paul Ehimare Aikpokpodion, [b] Raja Muthuramalingam Thangavelu, [b] Christian O. Dimkpa *[b] and Emeka Emmanuel Oguzie *[a]

Since the early 21st century, biochar (BC) has garnered attention for its agricultural and environmental applications. Water hyacinth (WH; *Eichhornia crassipes*), an invasive aquatic weed, has emerged as a promising feedstock for BC production due to its rapid growth and nutrient accumulation properties. However, studies on nano-nutrient fortification of WH-derived BC and the molecular dynamics of nutrient sorption remain limited. This study prepared BC from WH leaf (D1) and stem (D2) biomasses, achieving yields of 31% and 34%, respectively, under pyrolysis at 600 °C. Furnace residence times of 15–60 minutes were evaluated, with optimal carbonization occurring at ≥30 minutes. SEM and FTIR analyses revealed highly porous structures with functional groups, including −COOH, −OH, C≡C, and −S≡O, predominantly in D1. The BC was alkaline (pH 10.7), with liming capacities of 14.76–28.94% cc$_{eq.}$, zeta potentials of −34 to −38 mV, and particle sizes of 146–583 nm. The 30 minute BC exhibited high nitrogen (34 550 ppm), phosphorus (56 ppm), and potassium (609 ppm) availability, alongside water-holding capacities of 1.58–2.26 g g^{-1}. This study highlights the unexploited potential of WH as a sustainable resource towards nano-enabled biofertilizer development, offering a solution for managing the plant's invasive spread, while simultaneously improving soil nutrient management and contributing to atmospheric carbon sequestration, with positive implications for climate change mitigation.

Sustainability spotlight

This research focuses on the valorization of water hyacinth (*Eichhornia crassipes*), an invasive aquatic plant that poses significant ecological and socioeconomic challenges globally. By converting this biomass into value-added products, specifically through the production of nanonutrient-fortified biochar, we aim to address multiple sustainability goals aligned with the United Nations Sustainable Development Goals (SDGs). The utilization of water hyacinth not only mitigates the adverse effects of its proliferation—such as reduced biodiversity, impaired water transport, and damage to infrastructure—but also contributes to sustainable, smart and precision agricultural practices. The development of nano-enabled fertilizers from biochar derived from water hyacinth represents a circular economy-approach, transforming an ecological menace into a resource while enhancing soil health and agricultural productivity. This aligns with SDG 2 (zero hunger), which aims to end hunger, achieve food security, and promote sustainable agriculture by improving nutrient availability in soils. Our investigation into optimum production temperature and residence time for functional biochar emphasizes environmentally friendly and energy efficient techniques (pyrolysis at 600 °C for 15–60 min, with 30 min being optimum). These conditions ensure efficient conversion of biomass and enhance nutrient retention and availability in soils, which will promote precision agriculture. Theoretically, this research extends to computational modeling using Material Studio Software to unravel the molecular interactions between nanonutrients and biochar, examining their sorption dynamics, a property which is critical for crafting efficient nanobiofertilizer. This work aims to optimize fertilizer formulations for improved plant nourishment, contributing to global food security and ecological balance. Furthermore, this research has the potential to create positive socioeconomic impacts by generating job opportunities in the production and application of these green fertilizers where this invasive plant is present. It aligns with SDG 8 (decent work and economic growth) by promoting economic development through sustainable agricultural practices and supports SDG 12 (responsible consumption and production) by ensuring that natural resources are used sustainably in agricultural systems. In conclusion, our work seeks to expand knowledge on the upcycling of non-food crop biomass, particularly using water hyacinth as feedstock. This approach will not only address the ecological impacts of this invasive species but also enhance agricultural sustainability, carbon sequestration with attendant climate bearings, environmental sustainability *via* reduction in the pollution associated with the use of commercial fertilizers, ultimately further contributing to SDGs #9, 11, 13, 14 & 17.

[a]Nanotechnology Research, Africa Center of Excellence in Future Energies and Electrochemical Systems (ACEFUELS), Federal University of Technology, Owerri, Nigeria. E-mail: emeka.oguzie@futo.edu.ng

[b]Department of Analytical Chemistry, The Connecticut Agricultural Experiment Station (CAES), New Haven, Connecticut 06511, USA. E-mail: christian.dimkpa@ct.gov

[c]Department of Chemistry, Federal University of Petroleum Resources Effurun, Nigeria

† Electronic supplementary information (ESI) available. See DOI: https://doi.org/10.1039/d5su00052a

1 Introduction

Agriculture is fundamental to global food security[1] however, the challenge of meeting the nutritional needs of an estimated 10 billion people by 2050 necessitates innovative, smart and sustainable solutions.[2–4] Conventional fertilizers, while effective in boosting crop yields, pose environmental risks, including pollution, soil degradation, and unsustainable resource use.[5] Consequently, there is a growing shift towards eco-friendly alternatives that enhance nutrient availability to plants while minimizing adverse environmental impacts.[6,7] Among these, biochar (BC), a readily tunable carbonaceous product of biogenic feedstocks thermochemically processed in a non-oxidative atmosphere, has emerged as a versatile composite material with various organic precursors such as animal wastes,[8] rice husk,[9,10] sugar cane bagasse,[11] wood residues,[12] and sewage sludge.[13] The selection of feedstock and the pyrolytic conditions for BC production are usually determined by the type of application envisaged.[10,14–16] Among many other applications, BC has found applications in soil fertility enhancement, water retention, and carbon sequestration, providing a multifaceted solution to various agricultural and environmental challenges.[17–19] BC nutrient adsorption, retention and desorption capacity depends on its physicochemical properties which can in turn be modified by: (a) feedstock material, (b) pyrolytic conditions *e.g.* temperature and time, (c) pre- or post-pyrolysis treatment *e.g.* addition of nanoparticles or surface-active agents.[20] Together all these modifications can help to reduce production losses and enhance the slow-release characteristics of the resulting biogenic fertilizer product.[21–25]

Water hyacinth (WH, *Eichhornia crassipes*), an invasive aquatic weed, offers a unique feedstock opportunity. While WH's rapid proliferation disrupts aquatic ecosystems,[26–28] obstructs waterways,[29–32] and fosters disease vectors,[26,33,34] its profound ability to competitively bioaccumulate nutrients from the aquatic ecosystem[35,36] presents a potential resource for biofertilizer development. Therefore, upcycling WH for agricultural purposes[32,37–39] transforms this ecological menace into a valuable bioresource, as further evidenced by its applications in wastewater treatment,[40] biofuels,[41–43] bioremediation,[44,45] composite adsorbents[46–48] and supercapacitor.[49,50]

Bio-nanofertilizers are innovative, eco-friendly fertilizers that combine nanotechnology and biotechnology to enhance plant nutrient uptake and improve soil health. They consist of nanoscale materials that offer benefits such as enhanced seed germination, improved soil quality, increased nutrient use efficiency, and pesticide residue degradation.[51,52] BC is a highly suitable component for bio-nanofertilizer formulation due to its ability to enhance soil structure and porosity, boost nutrient retention, and foster microbial growth. It also acts as a carbon sink, sequestering carbon in a stable form, which helps mitigate climate change by reducing greenhouse gases like nitrous oxide.[51,53] BC also improves soil water retention and has liming capacity which are desirable properties for plants in agro-ecological zones with drought-impact and acidic soils. BC also plays a pivotal role in nanonutrients adsorption as a composite matrix in the bio-nanofertilizer conjugate, thereby increasing nutrient availability.[32]

This study investigated WH-derived BC as a foundation for nano-fertilizer formulation. By analyzing the effects of pyrolysis residence time (15–60 minutes) at 600 °C on WH biomass, it evaluated the physicochemical properties of the resulting BC. Characteristics such as nutrient retention, desorption in soil and aqueous media, porosity, surface functional groups, liming potential, water holding capacity were assessed, with modifications including feedstock selection (stem or leaf biomass) with the aim of nanoparticle integration to further optimize performance. Using the IBI classification system,[54] the liming potentials, fertilizer values, carbon storage capacities and particle size ranges of BC samples were assessed.

In their previous work, authors have used meta-analysis of individual research works from five databases (Springer, Academia, Google Scholar, Science Direct and PubMed) on WH, BC and nanofertilizer (NF) since the turn of the century (2000–2024) to identify gaps in the literature.[32] The data revealed an upsurge in research publications on BC increasing from 339 for the first 5 years (2000–2004) to 71 996 in the last 5 years (2020–2024), and WH from 1415 to 9087 within the same period. Conversely, research publications on WH, BC and NF only increased from zero to 25.[32] Therefore, this work aims to explore BC derived from WH for the purposes of NF formulation. Consequently, to optimize energy use, the effect of furnace residence time (15–60 min) at a fixed temperature of 600 °C (ref. 55) on the formation and physicochemical properties of BC derived from WH stem and leaf biomass was assessed.

A limited number of studies have delved into the properties of BC from WH in relation to its potential application as nano-enabled biofertilizers. This study is novel as it, for the first time, reports on the evaluation of the plant fertilization potential of nano-enabled BC from WH as a function of inherent characteristics such as liming capacity, nutrient content, and water-holding capacity. Ultimately, this research aims to provide a basis for integrating the invasive WH into a valuable agricultural input management strategy, which can ultimately address two critical issues simultaneously: providing a green alternative to conventional fertilizers and controlling the spread of the invasive species, thereby creating circular economy and safeguarding the socioeconomic life of the local communities where the weed is prevalent. This will also create a direct carbon sequestration pathway to reduce atmospheric CO_2, with climate change ramifications.

2 Materials and methods

We show in this study that the process of upcycling WH for biochar production towards the development of nano-enabled biofertilizer is facile. This process is summarized in Fig. 1.

2.1 Sample collection and biochar preparation

Feedstock for BC preparation were aerial tissues of WH harvested from Ekpan River, Uwwie Area of Effurun in Delta State, Nigeria (latitude: 5° 33′ 18″ and longitude: 5° 44′ 42″). The
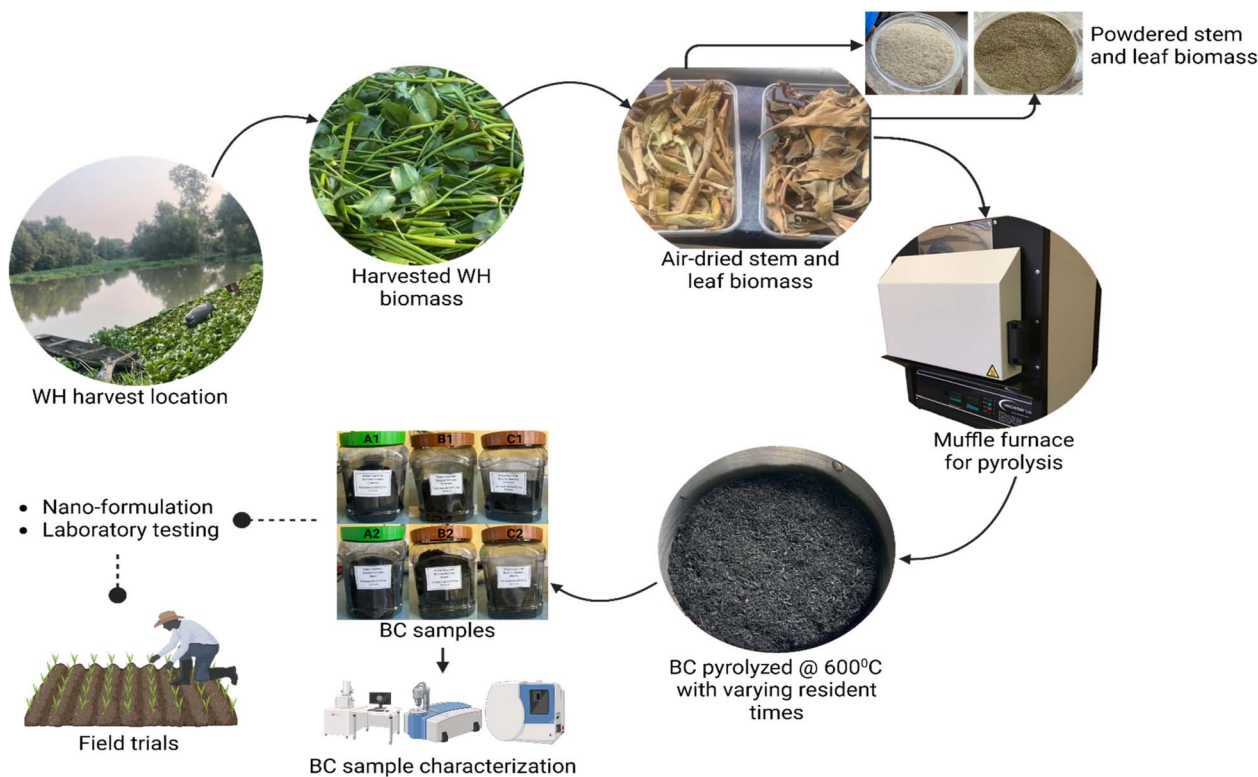
Fig. 1 Process summary for WH upcycling to produce BC for nano-enabled biofertilizer formulation.

samples were cleaned and separated into leaf and stem biomasses. Air-drying was carried out at ambient atmospheric conditions: temperature 30 °C, humidity 71%, and atmospheric pressure of 29.84 inHg until samples were dried to a consistent weight. The dry biomass was used in pyrolysis.

Dry WH leaf (D1) and stem (D2) biomasses were pyrolyzed at 600 °C (ref. 55) in oxygen deficient atmosphere for residence times of 15, 30, 45 and 60 min using a Vecstar muffle furnace model ECF2 (Vecstar Limited, Chesterfield, United Kingdom). The furnace temperature was set at 600 °C, increasing at 15 °C per min until the set temperature was attained and maintained for the pyrolysis residence time duration for each treatment. Pyrolyzed biomasses were allowed to cool to room temperature in airtight chambers to prevent oxidation. Biochar samples were thereafter milled and passed through a sieve with a 75 μm mesh pore to obtain consistent particle size range. Samples were labelled accordingly based on pyrolytic treatments. Biochar samples were kept in sealed labelled plastic containers for further analysis. Biochar yields were calculated for biomasses, D1 and D2 according to eqn (1):

$$Y_b = \frac{M_{bc}}{M_{bm}} \times 100\% \tag{1}$$

Y_b = biochar yield in percentage, M_{bc} = mass of biochar in grams, M_{bm} = mass of dry biomass in grams.

To assess the impact of pyrolytic treatments, the percentage nutrient concentration change (N_c) was calculated using the experimental biochar yield constant Y_b (0.31 and 0.34 for D1 and D2 biomass respectively) in eqn (2), with negative values

indicating possible nutrient loss during pyrolytic reactions while eqn (3) expresses the comparison of nutrient in biochar directly with biomass for each element.

$$N_c = \frac{N_B - (Y_b \times N_b)}{N_B} \times 100\% \tag{2}$$

For nutrient concentration impact of pyrolysis:

$$NC_i = \frac{N_b}{N_B} \times 100\% \tag{3}$$

where N_c = percentage nutrient concentration change during pyrolysis (%), N_B = nutrient content in biomass (g per 100 g of sample), Y_b = percentage biochar yield of biomass (%), N_b = nutrient content in biochar (g per 100 g of sample), NC_i = nutrient concentration impact of pyrolysis (%).

2.2 Biochar characterization

2.2.1 Elemental composition, morphological and surface property analyses. BC products were characterized for physico-chemical properties and determination of elemental constituents. Determination of elemental composition of samples was performed following the method described by Onorevoli *et al.*[56] Briefly, 0.25 g of samples were digested with 5 ml of 70% concentrated nitric acid (analytical grade) in 50 ml digestion tubes. Samples were then placed in a heating block set at 115 °C for 45 min. Digests were allowed to cool to ambient temperatures, diluted to 50 ml with de-ionized water and mixed to ensure homogeneity. Samples were allowed to settle for 2 h,

following which supernatants were taken from the digestates to determine elemental concentration using Inductively Coupled Plasma – Optical Emission Spectroscopy (ICP-OES) (iCap Pro, Qtegra Version 2.14.5122, Themo Fisher Scientific, MA).

Fourier Transform Infrared Spectroscopy with Attenuated Total Reflectance (FTIR-ATR) analysis was carried out using a Bruker Invenio-S instrument (Bruker Corporation, Billerica, Massachusetts, USA).[56,57] This technique was employed to detect functional groups and characterize the surface chemistry of both the WH biomass and the resulting BC products, with variations observed based on the pyrolytic conditions and the precursor biomass.

Sample morphology and relative elemental concentrations were analyzed with Scanning Electron Microscope Energy Dispersive X-ray Spectroscopy (SEM-EDX) using Hitachi SU3800/SU3900 Scanning Electron Microscopes (Hitachi High-Tech Corporation, Tokyo, Japan).[57,58] Each BC sample was placed on carbon tape and mounted on the sample holder. No specific pre-treatment was applied to the samples prior to SEM-EDX analysis because the inherent conductivity of carbon-based biochar minimizes charging effects, allowing it to perform well under electron diffraction conditions. The analysis was conducted using a Hitachi CFE SU8230 SEM at an accelerating voltage of 5 kV under high vacuum conditions. EDX was performed to assess the elemental composition of the biochar and trace elements. This non-destructive approach preserved the natural state of the biochar while providing comprehensive insights into its compositional characteristics. The SEM images were analyzed for porosity using python image analysis codes.

2.2.2 Determination of pH and liming potential. A 1 : 20 (w/v) sample/deionized water mixture was prepared by adding 0.25 g of samples (biochar: A1, B1, C1, A2, B2, C2 representing 30, 45 and 60 min pyrolyzed BC samples for D1 and D2 respectively, and biomass: D1 and D2) in test tubes and made up to 5 ml with deionized water. The mixtures were thoroughly mixed using a mechanical shaker for 15 min and allowed to equilibrate for 2 h, as previously reported.[59] The pH determination was done using pH meter Accumet Research (AR60; Fisher Scientific, USA).

The liming potential of the BC products was determined following the method described by Singh et al.[60] Briefly, 10 ml of a standard 1 mol per L HCl was added to 0.5 g of BC. The mixture was mechanically mixed for 30 min and was allowed to stand for 24 h. The resulting mixture was then back-titrated against a 0.5 mol per L NaOH solution ensuring continuous mixing until pH 7 is attained. Blank titration was carried out with 10 ml HCl without BC against the NaOH solution. The volumes of NaOH used were noted and the procedure repeated in triplicates. The liming potential was then expressed as percentage $CaCO_3$-equivalence (% $cc_{eq.}$) according to equation[4] and the classification used according to International Biochar Initiative (IBI) tool:[54]

$$\% \ cc_{eq.} = \frac{M \times (b - a) \times 10^{-3} \times 100.09 \times 100}{2 \times W} \quad (4)$$

M = molarity of NaOH (mol L^{-1}), b = volume of NaOH used in blank titration, a = volume of NaOH used in biochar sample

titration, 10^{-3} = for conversion of volume from ml to liters, 100.09 = molar mass of $CaCO_3$, 100 = multiplier for obtaining % $CaCO_3$ equivalence, W = mass of biochar (g), 2 = mole ratio number (1 mole of $CaCO_3$ consumes 2 moles of H^+).

2.2.3 Determination of zeta potential and hydrodynamic particle size. A Dynamic Light Scattering (DLS) Malvern Zeta sizer Ultra (Malvern Panalytical, Malvern, Worcestershire, United Kingdom) was used to determine net surface charges and hydrodynamic particle size of the BC products following the method used by Suliman[61] and Song et al.[62] Aqueous suspensions of the products were prepared by adding 2.5 mg of BC into 50 ml tubes and thoroughly mixing with deionized water. Samples were dispensed into Zeta sizer sample holders for net surface charge and hydrodynamic sizes determination.

2.2.4 Analysis of total nitrogen. Total nitrogen contents for the WH dry biomass (D1 and D2) and BC samples (A1, B1, C1, A2, B2, and C2) were analyzed with a LECO FP828 Nitrogen Determinator (LECO Corporation, Michigan, USA) using the method applied by Morais et al.[63] Nominal sample masses were weighed (0.10000–0.10999 g), wrapped in tin foil to form a capsule and then placed into the loader. The instrument then measures nitrogen content in the samples through combustion, capturing gaseous nitrogen that is delivered to a detector to ultimately generate percent nitrogen in the sample. Similarly, as shown by Morais et al.,[63] the percentage total nitrogen loss during pyrolysis can be calculated for each BC sample using the equation:

$$N_l = \frac{N_{bc} \times M_{bc}}{N_{bm} \times M_{bm}} \times 100\% \quad (5)$$

N_l = total nitrogen loss in percentage, N_{bc} = total nitrogen content in biochar after pyrolysis, M_{bc} = mass of biochar after pyrolysis, N_{bm} = total nitrogen content in biomass before pyrolysis, M_{bm} = mass of biomass before pyrolysis.

2.2.5 Biochar nutrient soil leaching test (nutrient release in soil medium). To test nutrient release in soil medium amended with BC products, 20 g of soil samples obtained from the Lockwood Farm in Hamden, Connecticut was amended with 2 g of BC samples at 10 : 1 (wt/wt).[64] The soil was thoroughly mixed with the BC and the mixture placed in a 50 ml sample tube. For the control, 20 g of soil without BC was used. 25 ml of deionized water was gently added to the soil–BC mixture and the control treatments, to obtain total leachates after 24 h. The leachates were collected daily for 5 days and kept at a temperature of 2 °C to prevent microbial degradation of the leachates prior to ICP OES analysis. Leachates were subsequently analyzed for elemental composition using ICP-OES, and for NH_4^+- and NO_3^--nitrogen using NH_4^+ and NO_3^- ion specific probes with a Hq Series multiprobe meter (Hach, Loveland, Colorado, USA).

2.2.6 Biochar nutrient release in aqueous medium. To assess experimentally the BC nutrient release in aqueous medium, 1 g of BC products were weighed into 14 ml plastic tubes. 10 ml of deionized water was gently added to the BC and allowed to equilibrate. The filtrate was allowed to drain through a filter to obtain total aqueous release after 24 h (ESI 1†). 10 ml of de-ionized water was added to the sample daily for 5 consecutive days and the aqueous samples obtained were

analyzed for elemental composition using ICP-OES, while NH_4^+- and NO_3^- – nitrogen determination was done using NH_4^+ and NO_3^- ion specific probes. Each sample was set up in triplicates.

2.2.7 Evaluation of biochar water holding capacity. Biochar water holding capacity (WHC) was evaluated based on the method described by Singh *et al.*[65] by weighing 1 g of BC sample into a 14 ml plastic tube. Next, 10 g of deionized water was gently added to the BC and the mixture allowed to soak completely. Water was allowed to drain out the hole at the bottom of the tube through a filter overnight and the recovered water was weighed and used to calculate the adsorbed water by the BC samples according to eqn (6):

$$WHC = \frac{(w_w - w_f)}{w_b} \times \frac{100}{1}\%$$ (6)

where w_w = weight of water added in g, w_f = weight of drained water after 24 h in g, w_b = weight of dry biochar sample in g.

2.2.8 Nitrate- and ammonium-nitrogen determination in leachate and aqueous release samples. NH_4NO_3 (analytical grade ≥98%; Sigma-Aldrich, USA) used in this study has a molar mass of 80.043 g mol^{-1} containing 62.049 g mol^{-1} of NO_3^- and 17.994 g mol^{-1} of NH_4^+. Therefore, 100 mg L^{-1} standard of NO_3^- solution was prepared by dissolving 0.0129 g of NH_4NO_3 in 100 ml of deionized water. Appropriate dilutions were then made to prepare 10 and 1 mg L^{-1} standards from the 100 mg L^{-1} standard respectively. Similarly, for NH_4^+ ions standard solution, 100 mg L^{-1} standard was prepared by dissolving 0.04448 g of NH_4NO_3 in 100 ml of deionized water. A 1 : 5 dilution was then made to prepare the 20 mg L^{-1} standard. These standards were used in calibrating the Hq series multiprobe meter used to determine the nitrate- and ammonium-nitrogen concentrations in the samples (see detailed explanation of calculations in ESI 2†).

2.2.9 IBI classification of BC samples. Determination of the value (or "grade") of the BC samples based on the International Biochar Initiative (IBI) classification system[54] is automatically estimated by inputting the following parameters into the online tool:

• Estimated hydrogen to organic carbon ratio (H/C_{org}) and organic carbon concentrations (C_{org}).

• Plant-available levels of phosphorus, potassium, sulfur, and magnesium as given by the total aqueous release over 5 days.

• Liming potential based on percentage calcium carbonate equivalent (% cc$_{eq.}$).

• Particle size distribution determined by hydrodynamic particle Zeta sizer.

With reference to Wei *et al.*,[66] estimated hydrogen to organic carbon ratio (H/C_{org}) from the SEM-EDX values were calculated and together with the plant-available (aqueous) levels of P, K, S, and Mg (see ESI 3†). The Biochar Classification Tool automatically computes and classifies biochars based on four input physicochemical properties as stated above. The output values from the tool are: carbon storage value, fertilizer value, liming value, and particle size distribution Table 1.[54]

Table 1 Pyrolysis yield, pH, liming capacity, carbon storage, particle size range and fertilizer value of BC from WH[a]

Water hyacinth biomass	Pyrolysis duration @ 600 °C	Biochar yield (%)	pH values	Liming capacity (% cc$_{eq.}$)		Fertilizer class	Carbon storage capacity (g kg^{-1})		Particle average size (nm)	
				Value	Class		Value	Class	Value	Class
Dry leaf samples (D1)	30 min (A1)	31.49 ± 1.04^a	10.77	28.94 ± 0.88^a	3	1	553	4	583	Fine powder
	45 min (B1)	31.48 ± 0.83^a	10.77	25.39 ± 0.57^b	3	1	469	3	354	Fine powder
	60 min (C1)	30.76 ± 0.65^a	10.61	23.85 ± 1.10^b	3	1	519	4	270	Fine powder
Dry stem samples (D2)	30 min (A2)	34.183 ± 1.28^b	10.71	22.60 ± 1.58^b	3	1	512	4	304	Fine powder
	45 min (B2)	34.066 ± 1.03^b	10.56	16.85 ± 0.96^c	2	1	474	3	146	Fine powder
	60 min (C2)	34.360 ± 0.98^b	10.72	14.76 ± 0.14^c	2	1	517	4	314	Fine powder

[a] Where applicable, values are given as means ± std error with lower case alphabets for significant differences at α = 0.05.

2.3 Statistical analysis

All experiments were set up in triplicates except where otherwise stated. Values are expressed as means and standard error ($\pm$SE). Significant differences were analyzed using a one-way ANOVA test with significant level set at $p < 0.05$ using the statistical package IBM SPSS Statistics 23.

3 Results and discussion

3.1 Biochar preparation and yield

Partial carbonization of the WH biomass was observed for $t = 15$ min, however, total pyrolysis was observed at 30, 45 and 60 min for D1 (leaf) and D2 (stem). Pyrolysis conditions, BC yield, pH and liming capacity data are shown in Table 1. BC yields from D1 are significantly lower than D2 ($p < 0.05$) for all the pyrolytic treatments indicating different biochemical composition of the WH leaf and stem as indicated by studies by (ref. 67). The higher BC yield observed from D2 can be explained from the presence of more fibrous and woody cellulose in the stem biomass with higher stable carbon content than D1 as previously shown,[67] where WH stem exhibited higher holocellulose, hemicellulose and cellulose than leaf biomass for WH from Yuriria Lake in Mexico. Additionally, both D1 and D2 showed yields consistent with results from (ref. 55, 68 and 69), where yields of between 33.6–51.8% were obtained with temperatures between 250–500 °C and residence time from 20 to 60 min. However, for D1 and D2, there are no significant differences in yield between the different pyrolytic residence times for each biomass type. Overall, the results highlight the influence of biomass type and biochemical composition on BC yield during pyrolysis with WH stems (D2) consistently produced significantly higher BC. Furthermore, the consistency in BC yields across varying pyrolytic residence times suggests that biomass composition, rather than duration, is the dominant factor in determining yield. These findings emphasize the critical role of feedstock selection in optimizing BC production for specific applications.

3.2 FTIR functional group characterization of WH biomass and biochar

FTIR data (Fig. 2) indicate that the functional groups present on the WH biomass and BC products varied based on the pyrolytic conditions and precursor biomass. For example, D1 spectra showed the presence of only amines, whereas A1, B1 and C1 show weak amine peaks with stronger nitro-groups being present. This could be due to oxidation of the amines to form nitro-compounds in the resulting BC products. On the contrary, A2, B2 and C2 do not show any peaks in the nitro- or amine-region, indicating the difference between the stem and leaf precursors. Alternatively, the amines in D2 could be more heat labile, effectively decomposing during the pyrolytic treatment. A summary of individual spectra is discussed subsequently,

D1: the WH leaf spectra shows a variety of functional groups typical of organic matter, including O–H, C–H, C=O, and C=C stretches, indicating the presence of alcohols, phenols, carboxylic acids, amines, and alkenes.
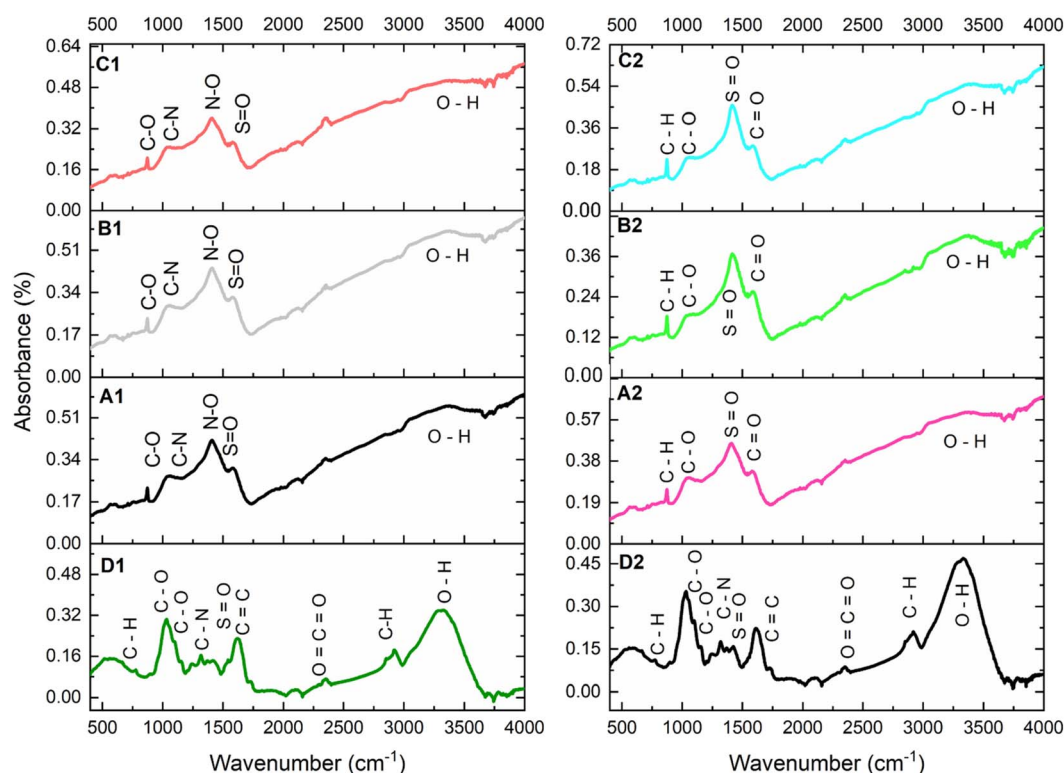

Fig. 2 FTIR spectra image qualified with absorbance (%) and wavenumber (cm^{-1}) for leaf biomass (D1) and biochar samples (A1, B1 and C1); stem biomass (D2) and biochar samples (A2, B2 and C2).

A1: the BC spectra show similar functional groups but with reduced intensity in the O–H stretch region, indicating some thermal degradation of organic compounds. The presence of sulfonyl and nitro groups suggests thermochemical changes during pyrolysis.

B1: the BC spectra is like A1, but with further reduction in the intensity of O–H stretches, indicating more extensive pyrolysis as residence time increased. The functional groups present indicate the progressive conversion of organic matter into more stable structures.

C1: the BC spectra is like B1 but with further reduced intensity in the O–H region and possibly higher carbonization, as indicated by the C=C stretches.

D2: the WH stem spectra shows a variety of functional groups typical of organic matter, including O–H, C–H, C=O, and C=C stretches, indicating the presence of alcohols, phenols, carboxylic acids, amines, and alkenes.

A2: the BC spectra shows similar functional groups but with reduced intensity in the O–H stretch region, indicating some thermal degradation of organic compounds. The presence of sulfonyl groups suggests chemical changes during pyrolysis.

B2: this spectrum is similar to A2, but with further reduction in the intensity of O–H stretches, indicating more extensive pyrolysis with residence time. The functional groups present indicate the progressive conversion of organic matter into more stable structures.
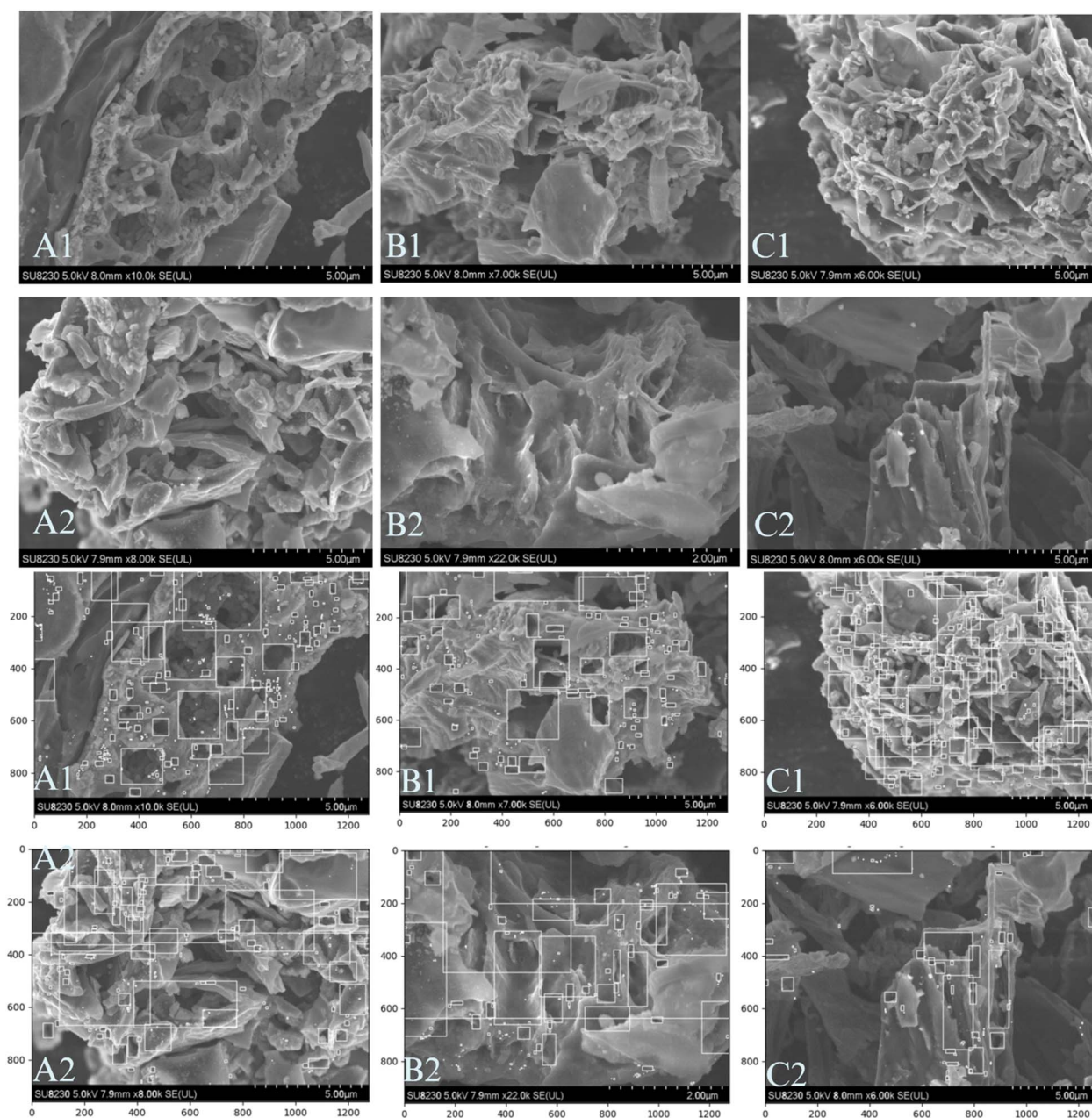

Fig. 3 Original SEM images taken with magnifications at ≥6000× (upper series) and SEM images with bounding boxes using python codes for pore analysis (lower series). A1: leaf biochar pyrolysed @ 30 min; B1: leaf biochar pyrolysed @ 45 min; C1: leaf biochar pyrolysed @ 60 min; A2: stem biochar pyrolysed @ 30 min; B2: stem biochar pyrolysed @ 45 min; C2: stem biochar pyrolysed @ 60 min.

C2: the BC spectra is similar to B2 but with further reduced intensity in the O–H region and possibly higher carbonization, as indicated by the C=C stretches.

As indicated by Li *et al.*,[70] the FTIR analysis underscores the transformative impact of pyrolytic conditions on the functional group composition of WH biomass. The distinct variations between D1 and D2 precursors highlight their biochemical diversity, with the former retaining amine functionality while the latter exhibits greater thermal lability. However, progressive pyrolytic residence time led to increased carbonization as indicated by the reduction in the O–H stretches and the formation of more aromatic, thermostable structures.[70] The pie-bonds in the aromatic species can be desirable for composite fortification especially with electrophilic nanonutrients.[71] However, the loss of surface functional groups such O–H and C–H at higher pyrolysis durations suggests a trade-off between the products' structural stability and adsorption properties,[72] which further underscores the need to select the optimum residence time for effective BC production. The findings point to a 30 minute pyrolysis as an optimal treatment for producing BC with balanced structural integrity and functional versatility, making it a promising candidate for nano-fortification in bio-fertilizer applications.

3.3 SEM-EDX characterization of WH biochar

SEM images of the BC are shown in Fig. 3 (top 2 rows) indicating variations in surface morphology and porosity with changing pyrolysis residence times for both D1 and D2. Subsequently, SEM images for the BC products at magnifications between 6000× and 22 000× were analyzed using python codes to estimate the pore sizes with bounding boxes (Fig. 3: bottom 2 rows). Estimated pore area sizes for the samples range from 0.03–0.46 μm^2. For a large hypothetical square nanoparticle of 100 nm by 100 nm size (0.1 μm by 0.1 μm), its area will be 10 000 nm^2 (0.01 μm^2). Therefore, as indicated by (ref. 73 and 74), extensive interfacial interactions both at the BC surface and within the micropores with nanoparticles will be feasible at the pore sizes with increased surface area for physisorption and chemisorption. It has been previously noted that BC structure becomes more ordered with higher porosity and increased surface area as pyrolytic residence time and temperature increases,[75–78] this is highly desirable for adsorption of nanonutrients for the purpose of fortifying the BC products for biofertilizer formulation. The micropores in BC products can also be beneficial as soil amendments for both water holding and aeration which can enhance soil properties for healthy plant growth.[78,79]

3.4 Hydrodynamic particle sizes and zeta potentials of BC

The hydrodynamic particle sizes and zeta potential measurements of biochar samples derived from WH biomass are crucial parameters for their potential application in nano biofertilizer formulation (Fig. 4). The average zeta sizes of the biochar samples indicate significant differences based on the biomass and pyrolytic treatments. D1-derived biochar samples exhibited larger particle sizes, with A1 at 583 nm, B1 at 354 nm, and C1 at 270 nm. Conversely, D2-derived biochar samples showed
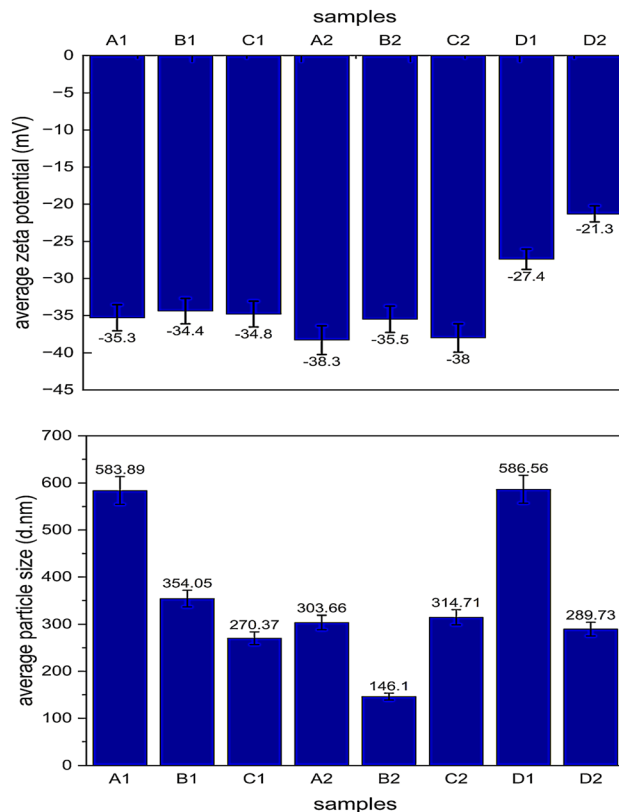

Fig. 4 Zeta sizes and zeta potentials of WH leaf, stem and biochar samples.

significantly smaller particle sizes, with A2 at 304 nm, B2 at 146 nm, and C2 at 314. These values are consistent with values obtained by Ha *et al.*,[80] when synthesizing NPK nanofertilizers using chitosan as the composite material with a size range between 300–700 nm. The zeta potential measurements of the biochar samples were consistently negative but significantly more negative than the feedstock biomass, D1 and D2. Specifically, the recorded values were −35 mV, −34 mV, −35 mV, −38 mV, −36 mV, and −38 mV for A1, B1, C1, A2, B2, and C2 respectively, consistent with the surface functional groups identified by FTIR. Such high negative zeta potential values indicate that the biochar particles possess a surface charge that can contribute to their colloidal stability in aqueous suspensions and subsequent nanoformulations. This stability is crucial for nano biofertilizer, as it will reduce the potential for the aggregation of particles, ensuring a uniform distribution of the biofertilizer when in liquid suspension.[62,81,82]

3.5 BC pH, liming potential, carbon storage, particle size range and fertilizer value based on IBI classification

The pH of the biomass was slightly acidic at 6.43 and 6.61 for D1 and D2 respectively whereas all BC samples range between 10.56–10.77 (Table 1). These data agreed with those obtained by Gezahegn *et al.*[83] The alkaline pH can be attributed to the presence of inorganic oxides of K, Ca and Na which are formed with oxygen atoms from the biomolecules during pyrolysis. However, a better

characterization is the liming potential of the BC samples, which was expressed as percentage $CaCO_3$ – equivalence (% $cc_{eq.}$). According to Table 1, BC products from D1 have the highest liming potential with mean values at 28.94%; 25.39%; 23.85% for A1, B1 and C1 respectively. In contrast, BC samples derived from D2 show significantly lower liming potential with A2 significantly higher than B2 and C2 with values of 22.60%; 16.85% and 14.76% respectively ($p < 0.05$). These values are similar to the range of 17.7 to 33.0% reported by Gezahegn et al.[83] In our study, the 30 min pyrolysis residence time produced the highest liming potential in both D1 and D2 samples ($p < 0.05$). The significantly higher values for D1 when compared with D2 can be explained by the presence of alkali metals in the leaves resulting in higher oxides, carbonates, phosphate or silicates formation which confers liming effects on the BC products. Based on the liming potential values, they are classified into class 0 (% $cc_{eq.} < 1\%$), class 1 (1% $\leq$ % $cc_{eq.} \leq 10\%$), class 2 (10% $\leq$ % $cc_{eq.} \leq 20\%$) and class 3 (20% $\leq$ % $cc_{eq.}$)[65] with A1, B1, C1 and A2 in class 3 and B2 and C2 in class 2. This also supports 30 min as the optimum pyrolytic residence time for higher liming capacity, which can be beneficial as amendments for acidic soils[84–86] found in several agronomic zones around the world especially in parts of Asia, Africa, South America and the United States.[87–90] Generally, BC physicochemical properties depend on the pre-, post-, and actual-pyrolytic treatments; and feedstock biomass types.[91,92] These properties modify the overall fertilizer value of the resulting BC, which can also be used to guide the selection of the candidate BC products for further nano-fortification as fertilizers.

In this study, the International Biochar Initiative (IBI) classification system was used.[54] This classification uses the percentage concentration of 6 major nutrients (N, P, K, S, Ca, and Mg) in the BC samples as well as the available portions to plants, estimated via total aqueous nutrient release/desorption over 5 days in this study. Other factors used in the classification include liming capacity, carbon storage value (based on organic carbon (C) and H/C ratio) and particle size range. Under this IBI system, BC fertilizer values are classified as 4, 3, 2, 1, and 0 with 4 being the best (Table 1). Theoretically, fertilizer class higher than 1 is desirable as this implies more nutrients are available to the extent needed by plant, however, field trials will be needed to validate this as soil–BC interactions also play a role in qualitative and quantitative nutrient availability.[92] However, in terms of liming capacity, D1-derived BC samples and the 30 min treatment for D2 all fall within class 3 and 4. Carbon storage capacity of the BC samples was also highest for A1 samples at 553 g kg^{-1} of sequestered carbon (Table 1).

3.6 Effect of pyrolytic treatments on biochar nutrient concentration and total nitrogen content

For a BC product to be effective as a nano-biofertilizer composite material, it must retain most of its nutrients for subsequent nano-enabling and eventual nutrient release to nourish plants. As shown in Table 2, a summary of the effects of these elements on plants is given.[93]

Table 3 Showing total nitrogen and nitrogen loss percentage after pyrolysis[a]

Samples	Total nitrogen content (%)	Mass of biochar (g)	Mass of biomass (g)	Nitrogen loss (%)
A1	3.53	42	134	341
B1	3.38	36	114	327
C1	3.27	41	133	309
A2	3.38	22	64	134
B2	1.69	26	77	67
C2	1.57	25	72	63

[a] NB: total nitrogen content for D1 and D2 are 3.07% and 1.16% respectively, these values were used for nitrogen loss percentage calculation using eqn (5).

Table 2 Key functions of selected elements in plant growth and development

Elements	Key functions
N	Essential for chlorophyll production, leaf development, and overall vegetative growth. It is a key component of amino acids and proteins
P	Crucial for root development, energy transfer (ATP), and flower/seed formation. It enhances early plant establishment
K	Regulates water uptake, enzyme activation, and disease resistance. It also improves fruit and seed quality
S	Aids in protein synthesis, enzyme activity, and chlorophyll production. It is essential for plant metabolism
Cu	Involved in enzyme function, photosynthesis, and lignin formation in plant cell walls. Deficiency can cause stunted growth
Zn	Essential for enzyme activation, hormone production, and protein synthesis. It also regulates growth and development
Fe	Plays a key role in chlorophyll formation and electron transport in photosynthesis. Deficiency leads to chlorosis (yellowing leaves)
Mg	A central component of chlorophyll, necessary for photosynthesis. It also activates many plant enzymes
B	Supports cell wall formation, reproductive development, and sugar transport. Deficiency affects flower and fruit formation
Ca	Important for cell wall structure, root development, and membrane stability. It helps prevent disorders like blossom-end rot

The experiments on nutrient release in both aqueous and soil media were conducted in batch mode at 24 hour intervals. Daily nutrient release from the samples was analyzed to determine the release pattern over time. The released nutrients were further compared with standard plant requirements[93] and assessed for fertilizer value based on the International Biochar Initiative (IBI) classification system.[54] The data reveal an intriguing pattern where BC samples from both D1 and D2 showed the highest total nitrogen content in the order 30 min > 45 min > 60 min pyrolysis durations, while nitrogen loss followed the inverse trend (60 min < 45 min < 30 min) across both feedstocks (Table 3). This suggests nitrogen-containing biomolecules like proteins, amides, pyrimidines, and amines become increasingly labile with extended furnace residence time, as exemplified by sample A1 which paradoxically retained the highest total nitrogen content (3.53% wt/wt) despite a 341% total nitrogen loss. These observations align with Abd El-Azeim et al.,[94] who identified 30 min pyrolysis at lower temperatures as optimal for improvement of soil fertility and organic matter content. This data also indicates that an increase in pyrolysis time at 600 °C promotes the condensation of nitrogen containing species into more stable heterocyclic compounds while volatilizing the heat-sensitive biomolecules via gasification.[95] Additionally, the increase in the nitrogen concentration can also be due to reactions such as dehydration and decarbonizations.[96] The effect of pyrolysis on nitrogen and other selected elements (P, K, S, Cu, Zn, Mg, Fe, B and Ca) in the biochar compared to the biomass is summarized in Table 4 (see ESI 3†).

For the biomasses, D1 has significantly higher concentrations of N, P, S, B and Ca than D2 whereas the reverse is the case with K, Cu, Zn and Fe. There is no significant difference between the concentrations of Mg in both D1 and D2 which agreed with reports from Lara-Serrano et al.[67] Pyrolytic treatments significantly increased P, K, Zn, Fe Mg, B and Ca but significantly decreased S and Cu contents in the BC products for D1. However, for D2, pyrolysis increased concentrations of P, S, Mg, Zn, B, and Ca whereas it reduced concentrations of Fe and Cu. For D2, K concentration was significantly higher in the 60 min pyrolysis, with no significant difference for 45 min and a significant reduction in concentration for the 30 min treatment.

3.7 Soil leachate and aqueous elemental availability

Considering that the BC samples were being explored for their suitability for possible nano-augmentation in biofertilizer formulation, it was necessary to assess the availability of nutrients in aqueous and soil media, to ensure their bioavailability. Leaching studies indicated that the BC samples had significantly higher and controlled release of key macronutrients (NPK) from day 2 in the soil medium, over the period of the experiment, compared to soil without BC amendment (Fig. 5). As observed by,[97] controlled and sustained release of nutrient from nanofertilizer enhanced plant growth and reduced the consumption of agrochemicals, especially of nitrogen. Results also indicate BC, being alkaline, produced significantly lower NO$_3$-N in the leachates extract with higher NH$_4$-N availability,

Table 4 Showing concentrations in ppm of N, P, K, S, Cu, Zn, Mg, Fe, B and Ca in biomass and biochar samples[a]

Samples	N	P	K	S	Cu	Zn	Mg	Fe	B	Ca
A1	35 300.0 ± 57.74[g]	58.48 ± 0.45[e]	655.33 ± 4.85[c]	11.5 ± 0.07[f]	0.01 ± 0.00[a]	0.37 ± 0.00[e]	63.78 ± 0.50[e]	4.55 ± 0.03[g]	0.19 ± 0.0[e]	255.01 ± 1.94[d]
B1	33 800.0 ± 23.09[f]	56.17 ± 0.43[d]	649.32 ± 5.05[c]	10.5 ± 0.07[d]	0.01 ± 0.00[b]	0.36 ± 0.00[e]	56.9 ± 0.12[d]	3.47 ± 0.02[e]	0.18 ± 0.0[d]	258.81 ± 1.67[e]
C1	32 700.0 ± 57.74[e]	62.43 ± 0.10[f]	582.88 ± 2.81[b]	10.41 ± 0.01[d]	0.02 ± 0.00[c]	0.46 ± 0.00[f]	62.06 ± 0.40[b]	2.41 ± 0.01[c]	0.18 ± 0.0[d]	254.75 ± 1.05[d]
A2	33 800.0 ± 57.74[f]	64.22 ± 0.17[g]	584.53 ± 1.42[b]	10.87 ± 0.03[e]	0.02 ± 0.00[c]	0.46 ± 0.00[f]	59.79 ± 0.36[b]	2.13 ± 0.01[b]	0.17 ± 0.0[c]	254.45 ± 0.85[d]
B2	16 900.0 ± 57.74[c]	38.65 ± 0.27[c]	904.33 ± 4.68[d]	6.1 ± 0.03[b]	0.03 ± 0.00[d]	0.29 ± 0.00[d]	56.97 ± 0.17[c]	1.98 ± 0.01[a]	0.19 ± 0.0[e]	221.9 ± 1.18[c]
C2	15 700.0 ± 57.74[b]	38.97 ± 0.17[c]	950.49 ± 2.30[e]	6.31 ± 0.03[c]	0.03 ± 0.00[d]	0.28 ± 0.00[c]	63.89 ± 0.15[e]	2.94 ± 0.02[d]	0.2 ± 0.0[f]	213.18 ± 0.56[b]
D1	30 700.0 ± 57.74[d]	19.6 ± 0.13[b]	201.22 ± 0.98[a]	13.95 ± 0.09[g]	0.04 ± 0.00[e]	0.16 ± 0.00[a]	18.41 ± 0.11[a]	2.41 ± 0.03[c]	0.06 ± 0.0[b]	215.31 ± 1.01[b]
D2	11 600.0 ± 57.74[a]	15.22 ± 0.13[a]	922.28 ± 15.57[d]	5.77 ± 0.03[a]	0.06 ± 0.00[f]	0.18 ± 0.00[b]	18.52 ± 0.02[a]	4.1 ± 0.12[f]	0.05 ± 0.0[a]	108.82 ± 0.24[a]

[a] Values are given as means ± std error with lower case alphabets for significant differences at $\alpha = 0.05$.

this could be a good application for acidic soils.[98] The predominance of NH_4^+-N compared to NO_3^--N in the total amount of N in leachate is a positive point for the BC materials with respect to nitrogen loss from agricultural soils. Several research reports on nitrogen loss from fertilizer application indicated that, nitrogen was mainly leached in the form of NO_3^--N rather than NH_4^+-N. Wang and Li[99] reported the predominance of NO_3-N as the main form of nitrogen loss in soil while Aikpokpodion et al.[100] in their study reported 98% of total N loss was in the form of NO_3^--N whereas NH_4^+-N was less than 2% of total N leached. The predominance of NH_4^+-N in the leachate infers that the biochar materials are going to supply nitrogen to the soil in a form that is more retained in soil as a result of its cationic charge that makes it bind to the negatively charged soil colloids and clay surfaces. On the contrary, NO_3^--N with its anionic charge is highly mobile in soil solution and easily get leached. However, the ultimate fate of the biochar-supplied NH_4^+-N lies on the rate and pathway of nitrification of ammonium to nitrate via ammonium oxidation to nitrite by oxidizing bacteria in soils. Additionally, with a controlled release from the BC, the N-nutrients can be released at rates needed by the plants thereby preventing accumulation and possible losses.[101]

The trend of phosphorus release from the various BC products show that, except for the control, there was a spike in the release of phosphorus from the various biochar materials during day 2 of leaching exercise before a progressive decline in P release in day 3 to day 5. Between the first and second day of

the leaching experiment, sample A1 had a 37.94% increase in P supply from the BC while samples B1, C1, A2, B2 and C2 had 71.98, 14.79, 37.71, 40.97 and 79.29% increase in P supply respectively. The increased release of phosphorus on day 2 of leaching compared to day 1 was an indication of the ability of the micropores within the BC to accumulate nutrient elements which are subsequently released to plants in a controlled manner. Many micropores are present in the BC pore structures resulting in more than 80% of the pore volume.[102] Phosphorus released on day 1 might have been the portion of P adsorbed on the surface of the biochar particles while the increased P released on day two might have been a combination of desorbed P from the particle surfaces and the portion of P adsorbed within the macro and micropores of the BC. Though the surge in P release from the biochar on day 2 could apparently lead to higher P supply than needed by plant and subsequent fixation of excess P in soil, the alkaline nature of the BC will create an environment unsuitable for P fixation. Phosphorus fixation in soil is mainly due to bonding of P to soil clay and hydr(oxides) of Al, Fe and Mn under acidic soil conditions.[103] Under acidic soil condition, the hydr(oxides) of Al, Fe and Mn are readily available in soil solution and consequently bind to phosphorus in a chemical reaction which limits the availability of P for plant uptake. With the alkaline condition of the BC, the released P has lesser potential of being fixed and subsequently bioavailable for plant utilization. The common surge in P release from BC-amended soils on day 2 of the experiment may also be attributed to a reduction in other P-limiting factors. This is
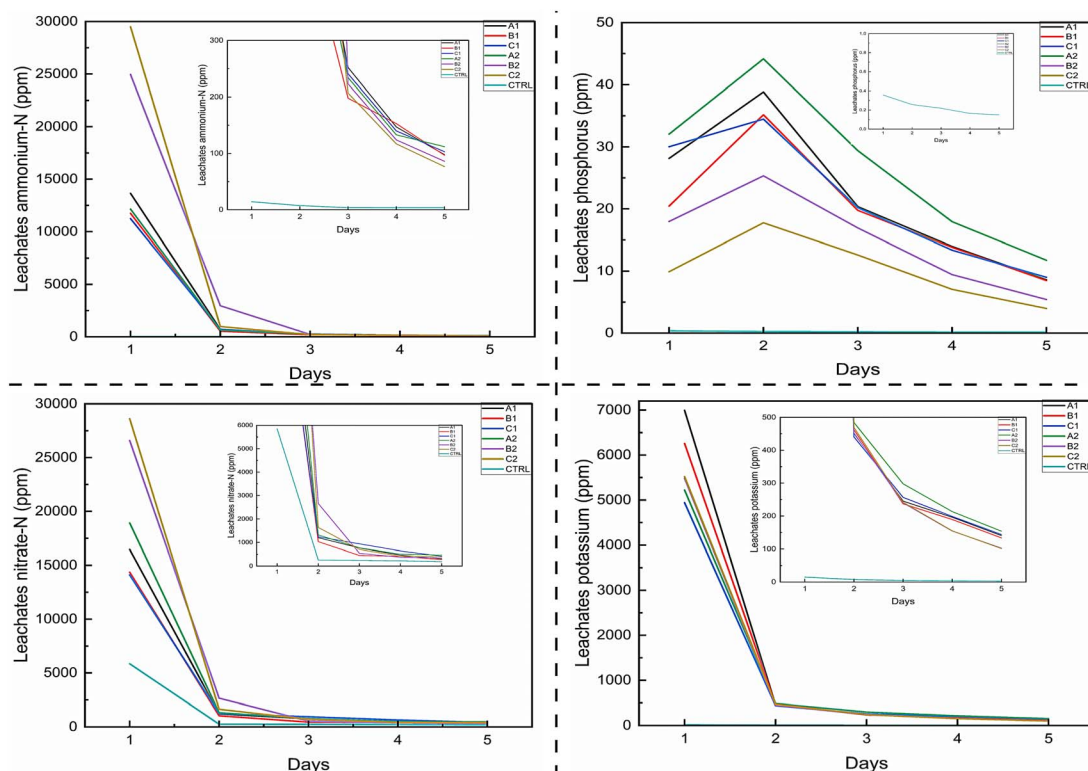

Fig. 5 Leachate concentrations showing continuous release of NH_4/NO_3-N, P, and K above the control soil without BC amendment over the period of the experiment (inserted graphs scaled to show trend vividly).

supported by findings from Wang *et al.*,[104] who showed that P release from BC decreases with an increase in certain anions (*e.g.*, NO_3^-, Cl^- and SO_4^{2-}), extended BC residence time in soils, and higher soil solution pH. These factors likely limited P availability on day 1, but their mitigation by day 2 led to a temporary increase in P release, which then gradually declined as the leaching experiment continued.

For K, release from soil amended with BC follow similar pattern with NO_3^--N and NH_4^+-N. Except for the control where the release continue to decrease over the period of the experiment, all BC-amended soil samples had a sharp decrease in K released from day 1 to day 2 of 93.54, 92.62, 91.07, 90.73, 91.74, 91.48% for A1, B1, C1, A2, B2, and C2 respectively as against a decrease of 46.67% by the control. This indicates K is readily available at significantly higher values in amended soils than the control. Doulgeris *et al.*[105] found similarly that increasing proportions of biochar amendment in soils resulted into doubling of available K, suggesting that this is enhanced by factors such as cation kinetic and equilibrium exchange.[105]

The detailed statistical analysis supporting these results are presented in ESI 4.†

3.8 Water holding capacity (WHC)

Water holding capacity (WHC) indicate an important property of the biochar for improvement of soil health for improved crop productivity. BC has been demonstrated to help alleviate plant's environmental stressors associated with water household such as drought and salinity.[106] For the leaf biochar samples, WHC decreased with pyrolysis residence time although A1 and B1 are not significantly different, both were significantly higher than C1. The reverse trend is observed with the stem-derived (D2) biochars where the WHC increased with pyrolytic residence time with A2 significantly lower than both B2 and C2 as shown in Fig. 6. High WHC is desirable as added benefits for biochar-based formulations and would ensure water and nutrients are available to plants while also enhancing the microbial activities within the soil microbiome as shown by Ghorbani *et al.* who found that biochar amendments enhanced water retention in soils and significantly increased rice yields under evaporation stress.[107] By reducing the amount of suction force required by plants to extract water from the soil, BC can positively modulate

plant's physiological and biochemical process thereby promoting plants' resilience and yields.[106–109]

4 Conclusions

This study is novel in highlighting, for the first time, the plant fertilization potential of BC from WH as a function of several inherent characteristics, including liming capacity, nutrient content, and water-holding capacity, among others. The findings show that water hyacinth (WH) can be a useful resource for soil amendment and its value in this regard can be further improved with nano fortification with micronutrients like Zn, Cu, B or Fe that are low in the biomass feedstock harvested from Ekpan River in Delta State, Nigeria. These micronutrients are known to have high adsorption ability to plant biomasses (110). Notably, pyrolytic treatments at 600 °C showed 30 min residence time as the optimum for both leaf and stem (D1 and D2) samples, indicating that these biomasses can be pooled during harvest to facilitate operations and subsequent downstream processing. This also is desirable in terms of energy requirements for the thermochemical treatment. With several desirable properties including liming capacity, water holding capacity, high concentration of available N, P, K and highly porous structure of the BC derived from WH, these products show promise for use in amendment in acidic and drought impacted soils. The carbon storage using this invasive plant for nano-biofertilizer formulation may be a way of synchronizing farming operations with natural autotrophic process by using this as a means of mining plant nutrients from water bodies *via* water hyacinth. This can be a double-edged advantage helping to capture and sequester atmospheric CO_2 through biochar-soil amendments since results in this study showed carbon content in biochar averaged above 70%.

The findings from this research will contribute to the development of environmentally friendly and economically viable solutions for sustainable agriculture and ecosystems preservation. Furthermore, WH derived BC can be a more balanced single fertilizer product than most commercial synthetic fertilizers. For example, urea, the most popular N fertilizer contains 46% N; TSP, the most popular phosphorus fertilizer contains 20% P, and MOP, the most popular K fertilizer contains 60% K. Although, effectively, not all these nutrients are available to the plant when applied, however, in contrast, BC products in this study released quantities of these macronutrients in soil medium above the required ppm by plants. Additionally, fortifying the biochar with nanoscale Cu and Zn that are known to be both nutrients and crop protection materials will broaden the functionality of the formulated nano-enabled fertilizer.

As previously discussed,[90] innovative fertilizers with balanced nutritional composition have the prospect of addressing multiple good public services, including waste management, climate change mitigation, and reduction of environmental pollution. Taken together, this work contributes to the development of environmentally friendly and economically viable fertilizer solutions for sustainable agriculture and ecosystems preservation, ultimately contributing to SDGs #8, 9, 11, 12, 13, 14 & 17. Further work is currently ongoing on further optimization of pyrolysis
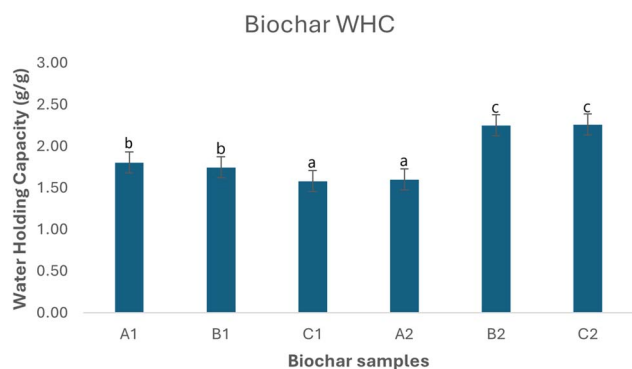

Biochar WHC

Fig. 6 Water holding capacity (WHC) of BC samples. Lower case letters denote significant differences ($\alpha = 0.05$).

conditions, focusing on temperature and biomass residence time, to produce functional biochar with minimal energy consumption and processing time. Additionally, experimental and computational molecular simulations are being conducted to study the sorption interactions between biochar and nano-nutrients. This research ultimately aims to fortify biochar with nanoscale nutrients to address elemental deficiencies in the feedstock, creating balanced nutrient products with the nano-enabled biochar-based fertilizers being tested on crops under field conditions to evaluate their effectiveness.

Data availability

Materials used and data associated with the research are available upon request.

Author contributions

Adewale T. Irewale: conceptualization; methodology; formal analysis and investigation; funding acquisition; writing—original draft preparation, review and editing. Elias E. Elemike: conceptualization; methodology; supervision; writing—review. Paul E. Aikpokpodion: methodology; statistical analysis; writing—review. Raja M. Thangavelu:: methodology; writing—review and editing. Christian O. Dimkpa: conceptualization; methodology; co-supervision; resources; funding acquisition; writing—review and editing. Emeka E. Oguzie: conceptualization; methodology; co-supervision; funding acquisition; validation.

Conflicts of interest

The authors claim there are no competing interests.

Acknowledgements

References

1 P. S. Bindraban, C. O. Dimkpa, S. Angle and R. Rabbinge, Unlocking the multiple public good services from balanced fertilizers, *Food Secur.*, 2018, **10**(2), 273–285.

2 R. Raliya, V. Saharan, C. Dimkpa and P. Biswas, Nanofertilizer for Precision and Sustainable Agriculture: Current State and Future Perspectives, *J. Agric. Food Chem.*, 2018, **66**(26), 6487–6503.

3 H. C. J. Godfray, J. R. Beddington, I. R. Crute, L. Haddad, D. Lawrence, J. F. Muir, *et al.*, Food Security: The Challenge of Feeding 9 Billion People, *Science*, 2010, **327**(5967), 812–818.

4 G. N. G. Saritha, T. Anju and A. Kumar, Nanotechnology - Big impact: How nanotechnology is changing the future of agriculture?, *J. Agric. Food Res.*, 2022, **10**, 100457.

5 A. T. Irewale, C. Dimkpa, F. O. Agunbiade, O. A. Oyetunde, E. E. Elemike and E. E. Oguzie, Unlocking Sustainable Agricultural Development in Africa via Bio-Nanofertilizer Application-Challenges, Opportunities and Prospects, *Sci. Afr.*, 2024, **25**, e02276. Available from: https://linkinghub.elsevier.com/retrieve/pii/S2468227624002217.

6 A. Nongbet, A. K. Mishra, Y. K. Mohanta, S. Mahanta, M. K. Ray, M. Khan, *et al.*, Nanofertilizers: A Smart and Sustainable Attribute to Modern Agriculture, *Plants*, 2022, **11**(19), 2587.

7 S. Garg, N. P. Rumjit and S. Roy, Smart agriculture and nanotechnology: Technology, challenges, and new perspective, *Adv. Agrochem*, 2024, **3**(1), 115–125.

8 L. N. Côrtes, S. P. Druzian, A. F. M. Streit, M. Godinho, D. Perondi, G. C. Collazzo, *et al.*, Biochars from animal wastes as alternative materials to treat colored effluents containing basic red 9, *J. Environ. Chem. Eng.*, 2019, **7**(6), 103446.

9 K. Nagaraju, T. N. V. K. V. Prasad, M. V. S. Naidu, M. S. Chari, Y. R. Ramu and B. R. Murthy, Exploring the Benefits of Rice Husk Waste: Synthesis and Characterization of Biochar and Nanobiochar for Agricultural and Environmental Sustainability, *Int. J. Environ. Clim. Change*, 2023, **13**(9), 715–725.

10 B. Bushra and N. Remya, Biochar from pyrolysis of rice husk biomass—characteristics, modification and environmental application, *Biomass Convers. Biorefin.*, 2024, **14**(5), 5759–5770.

11 C. Nie, X. Yang, N. K. Niazi, X. Xu, Y. Wen, J. Rinklebe, *et al.*, Impact of sugarcane bagasse-derived biochar on heavy metal availability and microbial activity: A field study, *Chemosphere*, 2018, **200**, 274–282.

12 J. Jiang, L. Zhang, X. Wang, N. Holm, K. Rajagopalan, F. Chen, *et al.*, Highly ordered macroporous woody biochar with ultra-high carbon content as supercapacitor electrodes, *Electrochim. Acta*, 2013, **113**, 481–489.

13 Anupama and P. Khare, A comprehensive evaluation of inherent properties and applications of nano-biochar prepared from different methods and feedstocks, *J. Cleaner Prod.*, 2021, **320**, 128759.

14 S. Alfei and O. G. Pandoli, Bamboo-Based Biochar: A Still Too Little-Studied Black Gold and Its Current Applications, *J. Xenobiot.*, 2024, **14**(1), 416–451.

15 A. E. D. Mahmoud and S. Kathi, Assessment of biochar application in decontamination of water and wastewater, in *Cost Effective Technologies for Solid Waste and Wastewater Treatment*, Elsevier, 2022, pp. 69–74.

16 K. Vijayaraghavan and R. Balasubramanian, Application of pinewood waste-derived biochar for the removal of nitrate and phosphate from single and binary solutions, *Chemosphere*, 2021, **278**, 130361.

17 R. k. Xu, N. P. Qafoku, E. Van Ranst, J. y. Li and J. Jiang, Adsorption Properties of Subtropical and Tropical Variable Charge Soils: Implications from Climate Change and Biochar Amendment, in *Advances in Agronomy*, 2016, pp. 1–58.

18 M. Mazarji, M. T. Bayero, T. Minkina, S. Sushkova, S. Mandzhieva, A. Tereshchenko, *et al.*, Realizing United Nations Sustainable Development Goals for Greener Remediation of Heavy Metals-Contaminated Soils by Biochar: Emerging Trends and Future Directions, *Sustainability*, 2021, **13**(24), 13825.

19 H. Xia, M. Riaz, M. Zhang, B. Liu, Y. Li, Z. El-Desouki, *et al.*, Biochar-N fertilizer interaction increases N utilization efficiency by modifying soil C/N component under N fertilizer deep placement modes, *Chemosphere*, 2022, **286**, 131594.

20 S. H. Bai, M. B. Farrar, M. Gallart, F. Reverchon, S. Taherymoosavi and N. Omidvar, *et al.*, Biochar effects on nutrient leaching, in *Biochar for Environmental Management*, Routledge, London, 2024, pp. 489–511.

21 L. Zheng, Y. Gao, J. Du, W. Zhang, Y. Huang, L. Wang, *et al.*, A novel, recyclable magnetic biochar modified by chitosan–EDTA for the effective removal of Pb(ii) from aqueous solution, *RSC Adv.*, 2020, **10**(66), 40196–40205.

22 A. Tomczyk and K. Szewczuk-Karpisz, Effect of Biochar Modification by Vitamin C, Hydrogen Peroxide or Silver Nanoparticles on Its Physicochemistry and Tetracycline Removal, *Materials*, 2022, **15**(15), 5379.

23 R. Ahuja, A. Kalia, R. Sikka and C. P, Nano Modifications of Biochar to Enhance Heavy Metal Adsorption from Wastewaters: A Review, *ACS Omega*, 2022, **7**(50), 45825–45836.

24 Y. L. Yaphary, M. He, G. Lu, F. Zou, P. Liu, D. C. W. Tsang, *et al.*, Experiment and multiscale molecular simulations on the Cu absorption by biochar-modified asphalt: An insight into removal capability and mechanism of heavy metals from stormwater runoff, *Chem. Eng. J.*, 2023, **462**, 142205.

25 Z. Liu, Z. Xu, L. Xu, F. Buyong, T. C. Chay, Z. Li, *et al.*, Modified biochar: synthesis and mechanism for removal of environmental heavy metals, *Carbon Res.*, 2022, **1**(1), 8.

26 P. L. Bolorunduro, *Water hyacinth infestation: nuisance or nugget*, 2023, available from: **https://hdl.handle.net/1834/18836**.

27 P. J. Ashton, W. E. Scott and D. J. Steÿn, The chemical control of water hyacinth [Eichhornia crassipes (MART.) SOLMS], in *Water Pollution Research and Development*, Elsevier, 1981, pp. 865–82.

28 W. Su, Q. Sun, M. Xia, Z. Wen and Z. Yao, The Resource Utilization of Water Hyacinth (Eichhornia crassipes [Mart.] Solms) and Its Challenges, *Resources*, 2018, **7**(3), 46.

29 A. Sharma, N. K. Aggarwal, A. Saini and A. Yadav, Beyond biocontrol: Water hyacinth-Opportunities and challenges, *J. Environ. Sci. Technol.*, 2016, **9**(1), 26–48.

30 R. Basaula, H. P. Sharma, J. L. Belant and K. Sapkota, Invasive Water Hyacinth Limits Globally Threatened Waterbird Abundance and Diversity at Lake Cluster of Pokhara Valley, Nepal, *Sustainability*, 2021, **13**(24), 13700.

31 S. I. Lubembe, S. Okoth, B. Turyasingura, T. Oyugi, H. Ibarasa, K. Moenga, *et al.*, Water Hyacinth, an Invasive Species in Africa: A Literature Review, *East African Journal of Environment and Natural Resources*, 2023, **6**(1), 198–216. **https://journals.eanso.org/index.php/eajenr/article/view/1293**.

32 A. T. Irewale, C. O. Dimkpa, E. E. Elemike and E. E. Oguzie, Water hyacinth: Prospects for biochar-based, nano-enabled biofertilizer development, *Heliyon*, 2024, **10**(17), e36966.

33 I. Iqbal, Fighting With a Weed: Water Hyacinth and the State in Colonial Bengal, c. 1910-1947, *Environ. Hist.*, 2009, **15**(1), 35–59. **https://www.jstor.org/stable/20723705**.

34 L. A. Navarro and G. Y. Phiri, *Water hyacinth in Africa and the Middle East: A survey of problems and solutions*, ed. L. A. Navarro and G. Y. Phiri, International Development Research Centre, Canada, 2000, pp. 1–119, available from: **https://idrc-crdi.ca/en/book/water-hyacinth-africa-and-middle-east-survey-problems-and-solutions**.

35 S. Gopal and India Mongabay Online Platform, *Researchers innovate to make money out of water hyacinth*, 2018 [cited 2024 May 17], available from: **https://india.mongabay.com/2018/01/researchers-innovate-to-generate-money-out-of-water-hyacinth/**.

36 S. Vidya and L. Girish, Water Hyacinth as a green manure for organic farming, *International Journal of Research in Applied, Natural and Social Sciences*, 2014, **2**(6), 65–72. **https://www.impactjournals.us**.

37 M. Abd El-Azeim, Z. Salah and A. Hammam, Assessment of Water Hyacinth Biochar as a Soil Amendment for Sandy Soils, *Journal of Soil Sciences and Agricultural Engineering*, 2021, **12**(6), 431–444.

38 G. O. Adesina, W. B. Akanbi, O. S. Olabode and O. Akintoye, Effect of water hyacinth and neem based composts on growth, fruit yield and quality of cucumber (Cucumis sativus), *Afr. J. Agric. Res.*, 2011, **6**(31), 6477–6484.

39 S. L. R. Begum, S. M. M. S. Himaya and S. M. M. S. Afreen, Potential of Water Hyacinth (Eichhornia crassipes) as Compost and its Effect on Soil and Plant Properties: A Review, *Agric. Rev.*, 2022, **43**(1), 20–28.

40 Manju, S. Kumari, J. Sharma, S. Gupta, M. Kumar, S. Kumar, *et al.*, An Assessment of Cadmium Removal from Simulated Waste Water Using Leftover Biomass of Water Hyacinth Immobilized via Emericella nidulans, *J. Appl. Life Sci. Int.*, 2016, **8**(3), 1–10.

41 S. M. M. Shanab, E. A. Hanafy and E. A. Shalaby, Water Hyacinth as Non-edible Source for Biofuel Production, *Waste Biomass Valorization*, 2018, **9**(2), 255–264.

42 U. S. P. Uday, P. Choudhury, T. K. Bandyopadhyay and B. Bhunia, Classification, mode of action and production strategy of xylanase and its application for biofuel production from water hyacinth, *Int. J. Biol. Macromol.*, 2016, **82**, 1041–1054.

43 A. Bhattacharya and P. Kumar, Water hyacinth as a potential biofuel crop, *Electron. J. Environ., Agric. Food Chem.*, 2010, **9**(1), 112–122.

44 S. Alvarado, M. Guédez, M. P. Lué-Merú, G. Nelson, A. Alvaro, A. C. Jesús, *et al.*, Arsenic removal from waters by bioremediation with the aquatic plants Water Hyacinth (Eichhornia crassipes) and Lesser Duckweed (Lemna minor), *Bioresour. Technol.*, 2008, **99**(17), 8436–8440.

45 S. H. Elias, M. Mohamed, A. N. Ankur, K. Muda, M. Hassan, M. N. Othman, *et al.*, Water hyacinth bioremediation for ceramic industry wastewater treatment-application of rhizofiltration system, *Sains Malays.*, 2014, **43**(9), 1397–1403.

46 S. M. Kanawade and R. W. Gaikwad, Removal of Methylene Blue from Effluent by Using Activated Carbon and Water Hyacinth as Adsorbent, *Int. J. Chem. Eng. Appl.*, 2011, **2**(5), 317–319.

47 X. Chen, X. Chen, X. Wan, B. Weng and Q. Huang, Water hyacinth (Eichhornia crassipes) waste as an adsorbent for phosphorus removal from swine wastewater, *Bioresour. Technol.*, 2010, **101**(23), 9025–9030.

48 L. M. Madikizela, Removal of organic pollutants in water using water hyacinth (Eichhornia crassipes), *J. Environ. Manage.*, 2021, **295**, 113153.

49 A. Saning, S. Herou, D. Dechtrirat, C. Ieosakulrat, P. Pakawatpanurut, S. Kaowphong, *et al.*, Green and sustainable zero-waste conversion of water hyacinth (*Eichhornia crassipes*) into superior magnetic carbon composite adsorbents and supercapacitor electrodes, *RSC Adv.*, 2019, **9**(42), 24248–24258.

50 P. Chaijak and P. Michu, Modified Water Hyacinth Biochar as a Low-Cost Supercapacitor Electrode for Electricity Generation From Pharmaceutical Wastewater, *Pol. J. Environ. Stud.*, 2022, **31**(6), 5471–5475.

51 P. Gehlot, J. Yadav, D. Chittora, S. Meena, P. Meena and T. Jain, Biofertilizers, Bionanofertilizers and Nanofertilizers: Ecofriendly alternatives for crop production, *Journal of Mycopathological Research*, 2024, **62**(2), 241–259.

52 S. M. El-Bialy, M. E. El-Mahrouk, T. Elesawy, A. E. D. Omara, F. Elbehiry, H. El-Ramady, *et al.*, Biological Nanofertilizers to Enhance Growth Potential of Strawberry Seedlings by Boosting Photosynthetic Pigments, Plant Enzymatic Antioxidants, and Nutritional Status, *Plants*, 2023, **12**(2), 302.

53 S. Das and P. J. Kim, *Nano-biofertilizer for Sustainable Agriculture*, APBB, 2023, DOI: 10.56669/CDMA8114.

54 International Biochar Initiative (IBI), *Biochar Classification Tool*, 2024 [cited 2024 Jul 14], available from: https://biochar-international.org/resources/biochar-classification-tool/.

55 L. Bottezini, D. P. Dick, A. Wisniewski, H. Knicker and I. S. C. Carregosa, Phosphorus species and chemical composition of water hyacinth biochars produced at different pyrolysis temperature, *Bioresour. Technol. Rep.*, 2021, **14**, 100684.

56 B. Onorevoli, G. P. da Silva Maciel, M. E. Machado, V. Corbelini, E. B. Caramão and R. A. Jacques, Characterization of feedstock and biochar from energetic tobacco seed waste pyrolysis and potential application of biochar as an adsorbent, *J. Environ. Chem. Eng.*, 2018, **6**(1), 1279–1287.

57 C. H. Chia, B. Gong, S. D. Joseph, C. E. Marjo, P. Munroe and A. M. Rich, Imaging of mineral-enriched biochar by FTIR, Raman and SEM–EDX, *Vib. Spectrosc.*, 2012, **62**, 248–257.

58 B. S. Archanjo, M. E. Mendoza, M. Albu, D. R. G. Mitchell, N. Hagemann, C. Mayrhofer, *et al.*, Nanoscale analyses of the surface structure and composition of biochars extracted from field trials or after co-composting using advanced analytical electron microscopy, *Geoderma*, 2017, **294**, 70–79.

59 S. Rajkovich, A. Enders, K. Hanley, C. Hyland, A. R. Zimmerman and J. Lehmann, Corn growth and nitrogen nutrition after additions of biochars with varying properties to a temperate soil, *Biol. Fertil. Soils*, 2012, **48**(3), 271–284.

60 B. Singh, J. E. Amonette, M. Camps-Arbestain and R. S. Kookana, A biochar classification system and associated test methods, in *Biochar for Environmental Management*, ed. J. Lehmann and S. Joseph, Routledge, London, 2024, pp. 209–48.

61 W. Suliman, J. B. Harsh, N. I. Abu-Lail, A. M. Fortuna, I. Dallmeyer and M. Garcia-Perez, Modification of biochar surface by air oxidation: Role of pyrolysis temperature, *Biomass Bioenergy*, 2016, **85**, 1–11.

62 B. Song, M. Chen, L. Zhao, H. Qiu and X. Cao, Physicochemical property and colloidal stability of micron- and nano-particle biochar derived from a variety of feedstock sources, *Sci. Total Environ.*, 2019, **661**, 685–695.

63 E. G. d. Morais, C. A. Silva, S. Gao, L. C. A. Melo, B. C. Lago, J. C. Teodoro, *et al.*, Empirical Correlation between Electrical Conductivity and Nitrogen Content in Biochar as Influenced by Pyrolysis Temperature, *Nitrogen*, 2024, **5**(2), 288–300.

64 M. S. Cahill, T. Arsenault, T. H. Bui, N. Zuverza-Mena, A. Bharadwaj, K. Prapayotin-Riveros, *et al.*, Copper Stimulation of Tetrahydrocannabinol and Cannabidiol Production in Hemp (*Cannabis sativa* L.) Is Copper-Type, Dose, and Cultivar Dependent, *J. Agric. Food Chem.*, 2024, **72**(13), 6921–6930.

65 B. Singh, J. E. Amonette, M. Camps-Arbestain and R. S. Kookana, A biochar classification system and associated test methods, in *Biochar for Environmental Management*, Routledge, London, 2024, pp. 209–48.

66 L. Wei, Y. Huang, L. Huang, Y. Li, Q. Huang, G. Xu, *et al.*, The ratio of H/C is a useful parameter to predict adsorption of the herbicide metolachlor to biochars, *Environ. Res.*, 2020, **184**, 109324.

67 J. S. Lara-Serrano, O. M. Rutiaga-Quiñones, J. López-Miranda, H. A. Fileto-Pérez, F. E. Pedraza-Bucio, J. L. Rico-Cerda, *et al.*, Physicochemical Characterization of Water

Hyacinth (Eichhornia crassipes (Mart.) Solms), *Bioresources*, 2016, **11**(3), 7214–7223.

68 X. Jin, N. Chen-yang, Z. Deng-yin, G. Yan-hui, H. Qi-min, X. Yu-hong, *et al.*, Co-pyrolysis of rice straw and water hyacinth: Characterization of products, yields and biomass interaction effect, *Biomass Bioenergy*, 2019, **127**, 105281.

69 M. Narayanan, G. Kandasamy, S. Kandasamy, D. Natarajan, K. Devarayan, M. Alsehli, *et al.*, Water hyacinth biochar and Aspergillus niger biomass amalgamation potential in removal of pollutants from polluted lake water, *J. Environ. Chem. Eng.*, 2021, **9**(4), 105574.

70 S. Li and G. Chen, Thermogravimetric, thermochemical, and infrared spectral characterization of feedstocks and biochar derived at different pyrolysis temperatures, *Waste Manage.*, 2018, **78**, 198–207.

71 B. Chen, D. Zhou and L. Zhu, Transitional Adsorption and Partition of Nonpolar and Polar Aromatic Contaminants by Biochars of Pine Needles with Different Pyrolytic Temperatures, *Environ. Sci. Technol.*, 2008, **42**(14), 5137–5143.

72 M. Ahmad, S. S. Lee, X. Dou, D. Mohan, J. K. Sung, J. E. Yang, *et al.*, Effects of pyrolysis temperature on soybean stover- and peanut shell-derived biochar properties and TCE adsorption in water, *Bioresour. Technol.*, 2012, **118**, 536–544.

73 Q. Chen, J. Zheng, J. Xu, Z. Dang and L. Zhang, Insights into sulfamethazine adsorption interfacial interaction mechanism on mesoporous cellulose biochar: Coupling DFT/FOT simulations with experiments, *Chem. Eng. J.*, 2019, **356**, 341–349.

74 J. Xing, W. Dong, N. Liang, Y. Huang, M. Wu, L. Zhang, *et al.*, Sorption of organic contaminants by biochars with multiple porous structures: Experiments and molecular dynamics simulations mediated by three-dimensional models, *J. Hazard. Mater.*, 2023, **458**, 131953.

75 J. Sun, F. He, Y. Pan and Z. Zhang, Effects of pyrolysis temperature and residence time on physicochemical properties of different biochar types, *Acta Agric. Scand., Sect. B*, 2017, **67**(1), 12–22.

76 B. Zhao, D. O'Connor, J. Zhang, T. Peng, Z. Shen, D. C. W. Tsang, *et al.*, Effect of pyrolysis temperature, heating rate, and residence time on rapeseed stem derived biochar, *J. Cleaner Prod.*, 2018, **174**, 977–987.

77 N. Claoston, A. Samsuri, M. Ahmad Husni and M. Mohd Amran, Effects of pyrolysis temperature on the physicochemical properties of empty fruit bunch and rice husk biochars, *Waste Manage. Res.*, 2014, **32**(4), 331–339.

78 A. T. Irewale, E. E. Elemike, A. M. Shaik, C. O. Dimkpa and E. E. Oguzie, Theoretical and experimental insights into BET surface area and pore analysis of water hyacinth biochar: Prospects for efficient bio-nanofertilizer development, *MRS Adv.*, 2025, DOI: 10.1557/s43580-025-01248-1.

79 B. Glaser, D. McKey, L. Giani, W. Teixeira, G. di Rauso Simeone and J. Schneeweiß, *et al.*, Historical accumulation of biochar as a soil amendment, in *Biochar*

for Environmental Management, Routledge, London, 2024, pp. 15–55.

80 N. M. C. Ha, T. H. Nguyen, S. L. Wang and A. D. Nguyen, Preparation of NPK nanofertilizer based on chitosan nanoparticles and its effect on biophysical characteristics and growth of coffee in green house, *Res. Chem. Intermed.*, 2019, **45**(1), 51–63.

81 G. Liu, H. Zheng, Z. Jiang, J. Zhao, Z. Wang, B. Pan, *et al.*, Formation and Physicochemical Characteristics of Nano Biochar: Insight into Chemical and Colloidal Stability, *Environ. Sci. Technol.*, 2018, **52**(18), 10369–10379.

82 J. Stewart, T. Hansen, J. E. McLean, P. McManus, S. Das, D. W. Britt, *et al.*, Salts affect the interaction of ZnO or CuO nanoparticles with wheat, *Environ. Toxicol. Chem.*, 2015, **34**(9), 2116–2125.

83 A. Gezahegn, Y. G. Selassie, G. Agegnehu, S. Addisu, F. Asargew Mihretie, Y. Kohira, *et al.*, Pyrolysis temperature changes the physicochemical characteristics of water hyacinth-based biochar as a potential soil amendment, *Biomass Convers. Biorefin.*, 2025, **15**(3), 3737–3752.

84 M. Lewoyehu, Y. Kohira, D. Fentie, S. Addisu and S. Sato, Water Hyacinth Biochar: A Sustainable Approach for Enhancing Soil Resistance to Acidification Stress and Nutrient Dynamics in an Acidic Nitisol of the Northwest Highlands of Ethiopia, *Sustainability*, 2024, **16**(13), 5537.

85 S. V. Vassilev, D. Baxter, L. K. Andersen and C. G. Vassileva, An overview of the composition and application of biomass ash, *Fuel*, 2013, **105**, 19–39.

86 S. V. Vassilev, D. Baxter, L. K. Andersen and C. G. Vassileva, An overview of the composition and application of biomass ash. Part 1. Phase–mineral and chemical composition and classification, *Fuel*, 2013, **105**, 40–76.

87 C. Dimkpa, W. Adzawla, R. Pandey, W. K. Atakora, A. K. Kouame, M. Jemo, *et al.*, Fertilizers for food and nutrition security in sub-Saharan Africa: An overview of soil health implications, *Front. Soil Sci.*, 2023, **3**, 1123931–1123948.

88 C. O. Dimkpa, Soil properties influence the response of terrestrial plants to metallic nanoparticles exposure, *Current Opinion in Environmental Science & Health*, 2018, **6**, 1–8.

89 M. Bekunda, N. Sanginga and P. L. Woomer, Restoring Soil Fertility in Sub-Sahara Africa, in *Advances in Agronomy*, 2010, pp. 183–236.

90 H. P. Binswanger-Mkhize and S. Savastano, Agricultural intensification: The status in six African countries, *Food Policy*, 2017, **67**, 26–40.

91 J. A. Ippolito, L. Cui, C. Kammann, N. Wrage-Mönnig, J. M. Estavillo, T. Fuertes-Mendizabal, *et al.*, Feedstock choice, pyrolysis temperature and type influence biochar characteristics: a comprehensive meta-data analysis review, *Biochar*, 2020, **2**(4), 421–438.

92 J. K. Whalen, L. Ejack, S. Gul and L. L. Castro, Characteristics of biochar, in *Biochar for Environmental Management*, Routledge, London, 2024, pp. 183–207.

93 C. Dimkpa, P. Bindraban, J. E. McLean, L. Gatere, U. Singh and D. Hellums, Methods for Rapid Testing of Plant and Soil Nutrients, in *Sustainable Agriculture Reviews*, ed. E. Lichtfouse, 25th edn, 2017, pp. 1–43, available from: http://link.springer.com/10.1007/978-3-319-58679-3_1.

94 M. Abd El-Azeim, Z. Salah and A. Hammam, Assessment of Water Hyacinth Biochar as a Soil Amendment for Sandy Soils, *Journal of Soil Sciences and Agricultural Engineering*, 2021, **12**(6), 431–444.

95 P. Gao, D. Guo, C. Liang, G. Liu and S. Yang, Nitrogen conversion during the rapid pyrolysis of raw/torrefied wheat straw, *Fuel*, 2020, **259**, 116227.

96 S. Xu, J. Chen, H. Peng, S. Leng, H. Li, W. Qu, *et al.*, Effect of biomass type and pyrolysis temperature on nitrogen in biochar, and the comparison with hydrochar, *Fuel*, 2021, **291**, 120128.

97 M. I. D. Helal, M. M. El-Mogy, H. A. Khater, M. A. Fathy, F. E. Ibrahim, Y. C. Li, *et al.*, A Controlled-Release Nanofertilizer Improves Tomato Growth and Minimizes Nitrogen Consumption, *Plants*, 2023, **12**(10), 1978.

98 D. Zhang, M. Yan, Y. Niu, X. Liu, L. van Zwieten, D. Chen, *et al.*, Is current biochar research addressing global soil constraints for sustainable agriculture?, *Agric., Ecosyst. Environ.*, 2016, **226**, 25–32.

99 Z. H. Wang and S. X. Li, Chapter Three - Nitrate N loss by leaching and surface runoff in agricultural land: A global issue (a review), *Advances in Agronomy*, ed. D. L. Sparks, Academic Press, 2019, vol. 156, pp. 159–217, ISSN 0065-2113, ISBN 9780128175989, DOI: 10.1016/bs.agron.2019.01.007.

100 P. E. Aikpokpodion, B. S. Hsiao and C. O. Dimkpa, Mitigation of Nitrogen Losses in a Plant–Soil System through Incorporation of Nanocellulose and Zinc-Modified Nanocellulose, *J. Agric. Food Chem.*, 2024, **72**(31), 17295–17305.

101 S. Wang, Y. Liu, L. Chen, H. Yang, G. Wang, C. Wang, *et al.*, Effects of excessive nitrogen on nitrogen uptake and transformation in the wetland soils of Liaohe estuary, northeast China, *Sci. Total Environ.*, 2021, **791**, 148228.

102 K. Weber and P. Quicker, Properties of biochar, *Fuel*, 2018, **217**, 240–261.

103 P. E. Aikpokpodion, Dynamics of phosphorus fixation in selected tea cropped soils on the Mambilla Plateau in Taraba State, Nigeria, *Nigerian Journal of Pharmaceutical and Applied Science Research*, 2023, **12**(4), 10–18.

104 Y. Wang, Y. Lin, P. C. Chiu, P. T. Imhoff and M. Guo, Phosphorus release behaviors of poultry litter biochar as a soil amendment, *Sci. Total Environ.*, 2015, **512–513**, 454–463.

105 C. Doulgeris, Z. Kypritidou, V. Kinigopoulou and E. Hatzigiannakis, Simulation of Potassium Availability in the Application of Biochar in Agricultural Soil, *Agronomy*, 2023, **13**(3), 784.

106 C. Kammann and E. R. Graber, Biochar effects on plant ecophysiology, in *Biochar for Environmental Management*, Routledge, London, 2024, pp. 381–99.

107 M. Ghorbani, R. W. Neugschwandtner, P. Konvalina, H. Asadi, M. Kopecký and E. Amirahmadi, Comparative effects of biochar and compost applications on water holding capacity and crop yield of rice under evaporation stress: a two-years field study, *Paddy Water Environ.*, 2023, **21**(1), 47–58.

108 M. Sofy, H. Mohamed, M. Dawood, A. Abu-Elsaoud and M. Soliman, Integrated usage of arbuscular mycorrhizal and biochar to ameliorate salt stress on spinach plants, *Arch. Agron. Soil Sci.*, 2021, **68**(14), 2005–2026.

109 A. W. M. Mahmoud, M. M. Samy, H. Sany, R. R. Eid, H. M. Rashad and E. A. Abdeldaym, Nanopotassium, Nanosilicon, and Biochar Applications Improve Potato Salt Tolerance by Modulating Photosynthesis, Water Status, and Biochemical Constituents, *Sustainability*, 2022, **14**(2), 723.